Electronic Supplementary Material (ESI) for Journal of Materials Chemistry C

Supporting Information

Pentaphenylphenyl Substituted Quinacridone Exhibiting Intensive Emission in Both of Solution and Solid State

Chenguang Wang,[a] Kai Wang,[a] Qiang Fu,[b] Jingying Zhang,[a] Dongge Ma,[*b] Yue Wang[*a]

[a] State Key Laboratory of Supramolecular Structure and Materials, College of Chemistry, Jilin University, Changchun 130012, P. R. China. E-mail: yuewang@jlu.edu.cn.

[b] State Key Laboratory of Polymer Physics and Chemistry, Changchun Institute of Applied Chemistry, Chinese Academy of Sciences, Changchun 130022, P. R. China. E-mail: mdg1014@ciac.jl.cn

Experimental Section

Materials

N,N'-Di(n-octyl)-2,9-diiodoquinacridone (I-QA-I) was synthesized as we reported.[1] THF was distilled from sodium/benzophenone ketyl under nitrogen atmosphere immediately prior to use. Other starting materials were common commercial grade and used as received.

General Measurements

^{1}H NMR spectra were measured on Bruker Avance 500 MHz or Varian Mercury 300 MHz spectrometer with tetramethylsilane (TMS) or resided solvent peak as the internal standard. Mass spectra were recorded on a Autoflex Speed MALDI-TOF mass spectrometer. Elemental analyses were performed on a Vario Micro (Elementar) spectrometer. UV-vis absorption spectra were recorded by a Shimadzu UV-2550 spectrophotometer. The emission spectra were recorded by an Edinburgh FLS920 spectrometer. The absolute fluorescence quantum yields of solutions and films were measured on Edinburgh FLS920 (excited at 490 nm). Cyclic voltammetries were performed on a BAS 100W instrument with a scan rate of 100 mV s^{-1}. A three-electrode configuration was used for the measurement: a platinum electrode as the working electrode, a platinum wire as the counter electrode,

and an Ag/Ag^+ electrode as the reference electrode. A 0.1 M solution of tetrabutylammonium hexafluorophosphate (TBAPF) in CH_2Cl_2 or THF was used as the supporting electrolyte. Differential scanning calorimetric (DSC) measurements were performed on a NETZSCH DSC204 instrument at a heating rate of 10 ℃ min^{-1} under nitrogen. Thermogravimetric analyses (TGA) were performed on a TAQ500 thermogravimeter at a heating rate of 10 ℃ min^{-1} under nitrogen.

Theoretical Calculations

The ground state geometries were fully optimized by the DFT[2] method with the Becke three-parameter hybrid exchange and the Lee-Yang-Parr correlation functional (B3LYP)[3] and 6-31G* basis set using the Gaussian 03 software package.[4]

Device Fabrication and Measurement.

The hole-injection material poly-(3,4-ethylenedioxythiophene):poly-(styrenesulfonate) (PEDOT:PSS), electron-transporting material 1,3,5-tris(N-phenylbenzimidazol-2-yl)benzene (TPBi) were commercially available. Commercial ITO (indium tin oxide) coated glass with sheet resistance of 10 Ω per square was used as the starting substrates. Before device fabrication, the ITO glass substrates were precleaned carefully and treated by oxygen plasma for 2 min. PEDOT:PSS (40 nm) was first spin-coated to smooth the ITO surface and dried at 120 ℃ for 30 min under vacuum. Then the emissive layer of NPB:Alq3 (1:1) doped with 1 wt %, 3 wt % or 5 wt % BPP-QA (40−45 nm) was spin-coated from chlorobenzene solution onto the PEDOT: PSS layer and dried at 100 ℃ for 30 min to remove residual solvent. Finally, TPBi (35 nm), and a cathode composed of lithium fluoride (LiF, 1 nm) and aluminum (Al, 100 nm) were sequentially deposited onto the substrate by vacuum deposition in the vacuum of 10^{-6} Torr. The *J-V-L* of the devices was measured with a Keithley 2400 Source meter and a Keithley 2000 Source multimeter equipped with a calibrated silicon photodiode. The EL spectra were measured by JY SPEX CCD3000 spectrometer. All measurements were carried out at room temperature under ambient conditions.

Synthesis

N,N'-Di(n-octyl)-2,9-di(2-phenylethynyl)quinacridone (Pa-QA-Pa). To a two-neck flask, **I-QA-I** (600 mg, 0.761 mmol), $Pd(Pph_3)_4$ (44 mg, 0.038 mmol), CuI (36 mg, 0.188 mmol), refreshed THF (20 mL) and Et_3N (2 mL) was added. The mixture was degassed by a repeated procedure of freeze-pump-thaw and then phenylacetylene (0.186 mg, 1.82 mmol) was added. The mixture was refluxed for 12 hours under nitrogen atmosphere. After cooled to room temperature, the solvents were removed by rotary evaporator and the residual solid was purified by column chromatography (silica gel, petrol ether/CH_2Cl_2 1 : 1 to 1 : 5) to give orange-red solid **Pa-QA-Pa** (526 mg, 94%). ^{1}H NMR (300 MHz, $CDCl_3$): δ 8.60 – 8.54 (m, 4H), 7.76 (dd, *J* = 9.0 Hz, *J* = 2.1 Hz, 2H), 7.62 – 7.56 (m, 4H), 7.42 – 7.33 (m, 8H), 4.46 (t, *J* = 7.2 Hz, 4H), 2.02 – 1.90 (m, 4H), 1.67 – 1.56 (m, 4H), 1.52 – 1.27 (m, 16H), 0.91(t, *J* = 6.6 Hz, 6H). Ms m/z: 736.3 $[M]^+$ (calcd: 736.4). Anal.Calcd (%) for $C_{52}H_{52}N_2O_2$: C, 84.75; H, 7.11; N, 3.80. Found: C, 84.59; H, 7.32; N, 3.85.

BPP-QA. Under nitrogen atmosphere, the mixture of **Pa-QA-Pa** (470 mg, 0.638 mmol), tetraphenylcyclopentadienone (491 mg, 1.28 mmol) and diphenyl ether (10 mL) was refluxed for 24 h. After cooled to room temperature, the mixture was added into methanol (200 mL) and filtrated. The orange solid product **BPP-QA** (831 mg, 90%) was purified by column chromatography (silica gel, petrol ether/CH_2Cl_2, V:V = 1:1 to 1:5). ^{1}H NMR (500 MHz, $CDCl_3$): δ 8.58 (s, 2H), 8.06 (d, *J* = 2.0 Hz, 2H), 7.24 (dd, *J* = 9.0 Hz, *J* = 2.0 Hz, 2H), 7.00 (d, *J* = 9.0 Hz, 2H), 6.93 (d, *J* = 8.0 Hz, 4H), 6.88 – 6.81 (m, 42H), 6.76 (t, *J* = 7.5 Hz, 4H), 4.28 (t, *J* = 7.0 Hz, 4H), 1.83 – 1.73 (m, 4H), 1.46 – 1.39 (m, 4H), 1.39 – 1.25 (m, 16H), 0.91 (t, *J* = 7.0 Hz, 6H). Ms m/z: 1450.8 $[M]^+$ (calcd: 1449.7). Anal.Calcd (%) for $C_{108}H_{92}N_2O_2$: C, 89.47; H, 6.40; N, 1.93. Found: C, 89.76; H, 6.34; N, 1.92.

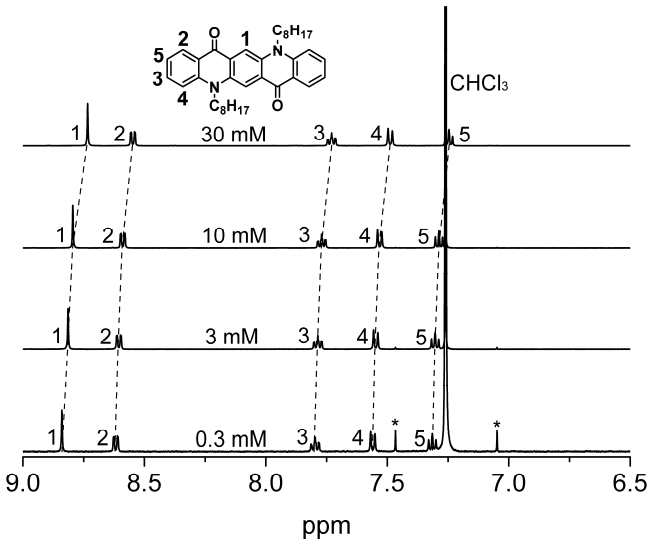

Fig. S1 Concentration-dependent ^{1}H NMR spectra of C8-QA in $CDCl_3$ at 25℃.

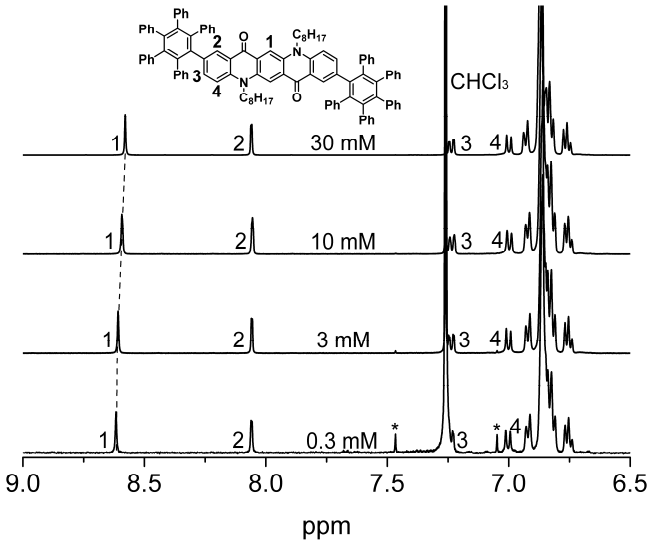

Fig. S2 Concentration-dependent ^{1}H NMR spectra of BPP-QA in $CDCl_3$ at 25℃.

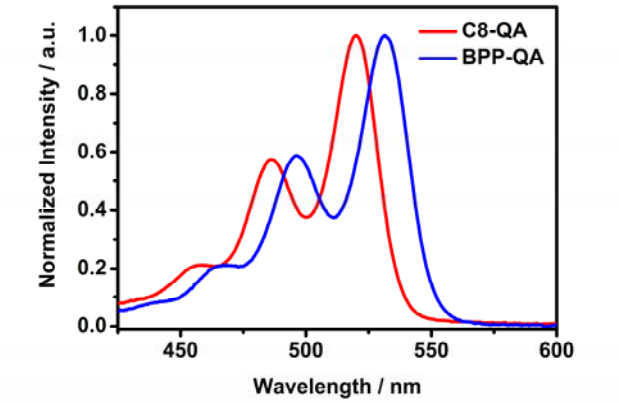

Fig. S3 The UV−visible absorption spectra of C8-QA and BPP-QA in dilute CH_2Cl_2 solutions (1 × 10^{-5} mol L^{-1}).

Table S1 Electrochemical data, HOMO/LUMO energy levels and thermal data of the compounds.

			Experimental data			DFT calculations			
Compound	$E_{ox}^{1/2}$ (V)[a]	$E_{red}^{1/2}$ (V)[a]	E_{HOMO} (eV)[b]	E_{LUMO} (eV)[b]	E_g^{CV} (eV)[c]	E_{HOMO} (eV)	E_{LUMO} (eV)	E_g^{DFT} (eV)[c]	T_m/T_d (℃)
C8-QA	0.69	–1.99	–5.79	–3.11	2.68	–5.25	–2.13	3.12	179/370
BPP-QA	0.60	–2.04	–5.70	–3.06	2.64	–5.06	–2.00	3.06	405/464

[a] Potentials were given against ferrocene/ferrocenium (Fc/Fc^+). [b] The HOMO levels were estimated from $E_{HOMO} = -(E_{ox}^{1/2} + 5.1)$ (eV); The LUMO levels were estimated from $E_{LUMO} = -(E_{red}^{1/2} + 5.1)$ (eV). [c] The energy gap were estimated from $E_g = E_{LUMO} - E_{HOMO}$ (eV).

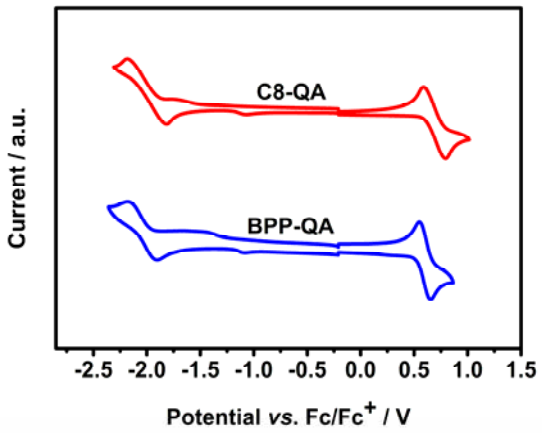

Fig. S4 Cyclic voltammograms of the compounds in THF (reduction) and CH_2Cl_2 (oxidation), measured with TBAPF (0.1 M) as a supporting electrolyte at a scan rate of 100 mV s^{-1}.

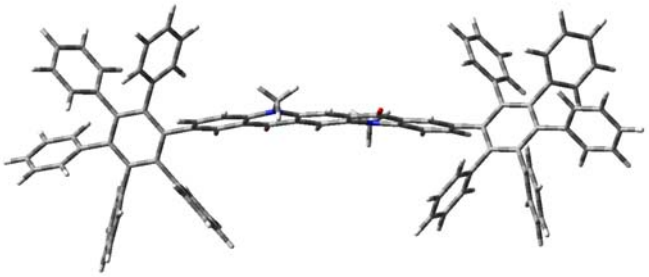

Fig. S5 The optimized molecular geometry of BPP-QA based on the B3LYP/6-31G* level.

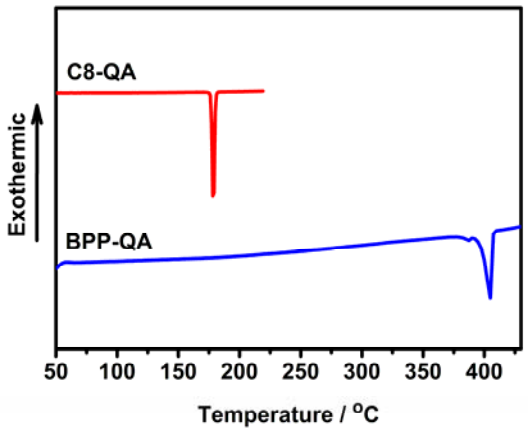

Fig. S6 DSC curves of the componds.

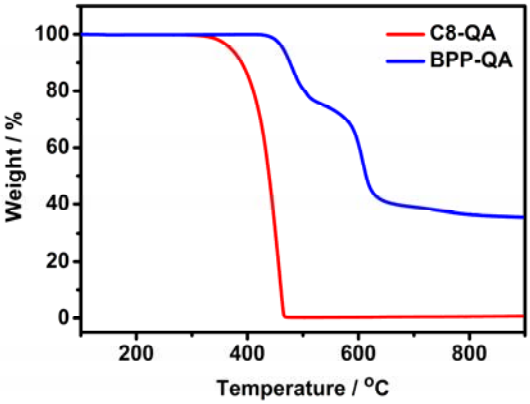

Fig. S7 TGA curves of the componds.

Table S2 EL performance of devices with different doping concentration of BPP-QA.

Doping concentration[a]	λ_{EL}[b] (nm)	V_{on}[c] (V)	L_{max}[d] (cd m^{-2})	η_c[e] (cd A^{-1})	η_p[f] (lm W^{-1})
1%	545	4.6	14163	6.4	3.8
3%	546	3.6	23458	10.0	7.1
5%	546	4	25896	8.0	5.3

[a] Device structure: [ITO/PEDOT:PSS (40 nm)/NPB:Alq$_3$:BPP-QA(x%) (40 nm)/TPBi (35 nm)/LiF (1 nm)/Al]; [b] Peak electroluminescence; [c] Turn-on voltage; [d] Maximum brightness; [e] Maximum current effeiciency. [f] Maximum power effeiciency.

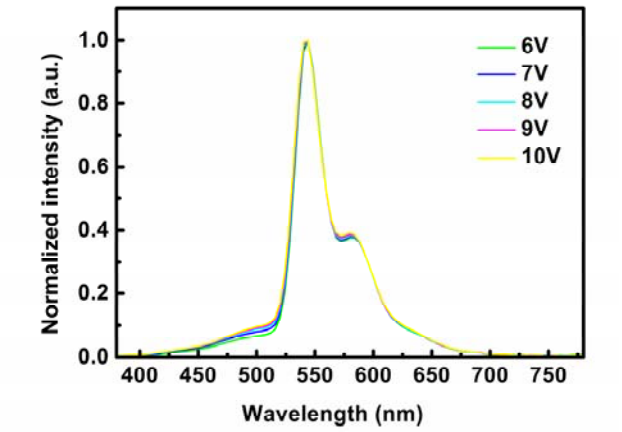

Fig. S8 The EL spectra of the device with doping concentration of 1% at different votages.

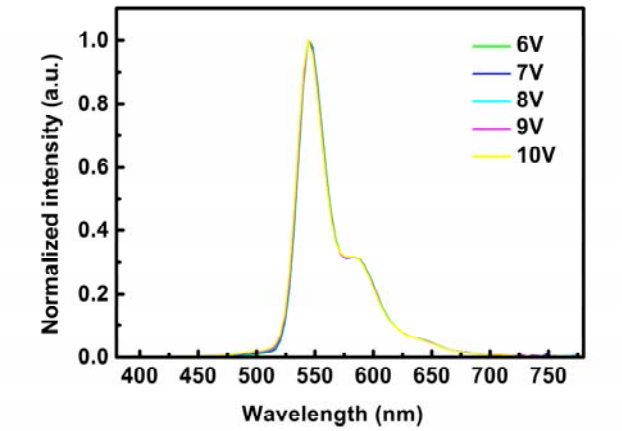

Fig. S9 The EL spectra of the device with doping concentration of 3% at different votages.

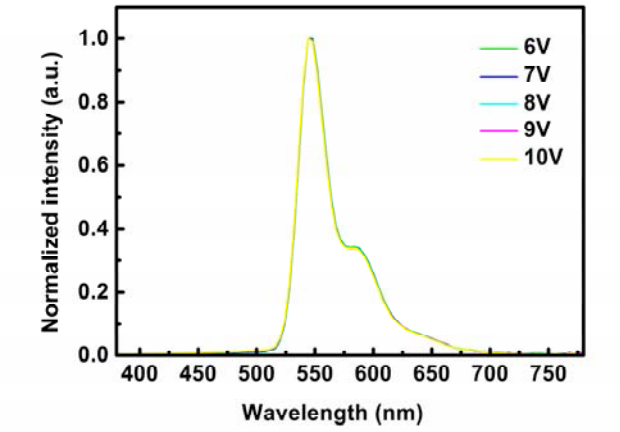

Fig. S10 The EL spectra of the device with doping concentration of 5% at different votages.

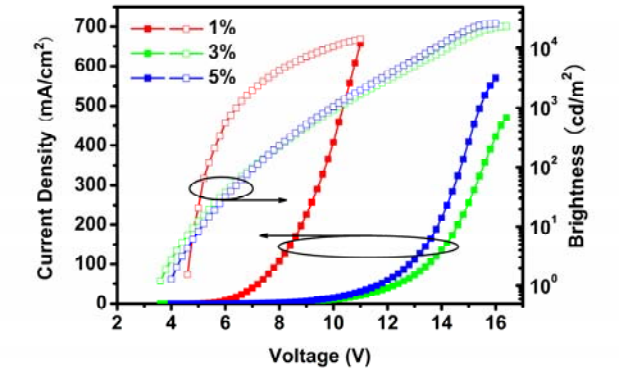

Fig. S11 Current density−voltage−luminance characteristics of the devices with doping concentration of 1%, 3% and 5%.

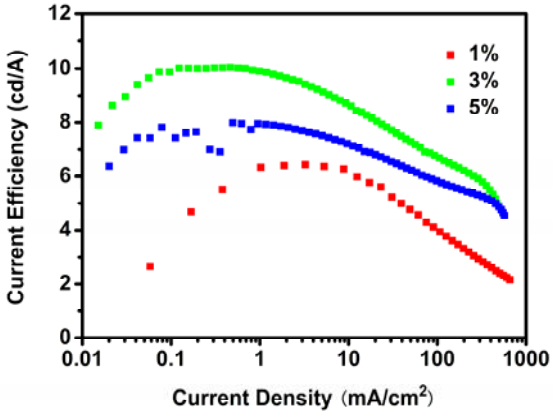

Fig. S12 Current efficiency versus current density of the devices with doping concentration of 1%, 3% and 5%.

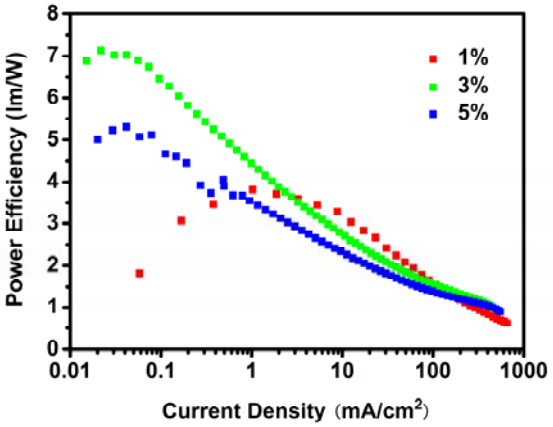

Fig. S13 Power efficiency versus current density of the devices with doping concentration of 1%, 3% and 5%.

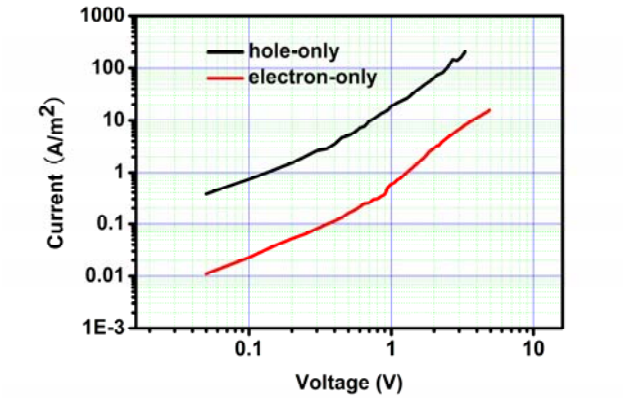

Fig. S14 Current−voltage curves of hole-only and electron-only devices. Hole-only device structure: [ITO/ PEDOT:PSS (40 nm)/ BPP-QA (100 nm)/ NPB (15 nm)/ Au], electron-only device structure: [Al/ BPP-QA (100 nm)/ TPBi (15 nm)/ LiF (1 nm)/ Al].

References

1 C. Wang, W. Chen, S. Chen, S. Zhao, J. Zhang, D. Qiu and Y. Wang, *New J. Chem.*, 2012, **36**, 1788.

2 E. Runge and E. K. U. Gross, *Phys. Rev. Lett.*, 1984, **52**, 997.

3 A. D. J. Becke, *Chem. Phys.*, 1993, **98**, 5648.

4 M. J. Frisch, G. W. Trucks, H. B. Schlegel, G. E. Scuseria, M. A. Robb, J. R. Cheeseman, J. A. MontgomeryJr., T. Vreven, K. N. Kudin, J. C. Burant, J. M. Millam, S. S. Iyengar, J. Tomasi, V. Barone, B. Mennucci, M. Cossi, G. Scalmani, N. Rega, G. A. Petersson, H. Nakatsuji, M. Hada, M. Ehara, K. Toyota, R. Fukuda, J. Hasegawa, M. Ishida, T. Nakajima, Y. Honda, O. Kitao, H. Nakai, M. Klene, X. Li, J. E. Knox, H. P. Hratchian, J. B. Cross, C. Adamo, J. Jaramillo, R. Gomperts, R. E. Stratmann, O. Yazyev, A. J. Austin, R. Cammi, C. Pomelli, J. W. Ochterski, P. Y. Ayala, K. Morokuma, G. A. Voth, P. Salvador, J. J. Dannenberg, V. G. Zakrzewski, S. Dapprich, A. D.

Daniels, M. C. Strain, O. Farkas, D. K. Malick, A. D. Rabuck, K. Raghavachari, J. B. Foresman, J. V. Ortiz, Q. Cui, A. G. Baboul, S. Clifford, J. Cioslowski, B. B. Stefanov, G. Liu, A. Liashenko, P. Piskorz, I. Komaromi, R. L. Martin, D. J. Fox, T. Keith, M. A. Al-Laham, C. Y. Peng, A. Nanayakkara, M. Challacombe, P. M. W. Gill, B. Johnson, W. Chen, M. W. Wong, C. Gonzalez, J. A. Pople, *Gaussian 03, Revision C.02*, Gaussian, Inc.: Pittsburgh, PA 2003.